ARCHIVES
of
FOUNDRY ENGINEERING

ISSN (2299-2944)
Volume 2026
Issue 1/2026

118 – 123

14/1

10.24425/afe.2026.157977

Published quarterly as the organ of the Foundry Commission of the Polish Academy of Sciences

Effect of Heat Treatment on the Strain Hardening Behaviour of an Al-Si-Cu Alloy

M. Frátrik *, E. Kantoríková
University of Žilina, Slovak Republic
* Corresponding author: E-mail address: martin.fratrik@fstroj.uniza.sk

Received 26.09.2025; accepted in revised form 07.01.2026; available online 30.03.2026

Abstract

This study investigates the mechanical behaviour of the AlSi9Cu1 alloy after T6 heat treatment, with a focus on its strain hardening response. Uniaxial tensile tests were conducted on heat-treated specimens to determine the strain hardening exponent n and the strength coefficient K. These parameters were subsequently used to assess the alloy's potential for strain strengthening during mechanical surface treatments such as roller burnishing, shot peening, and grit blasting. The results indicate that specimens subjected to artificial aging within the peak-aged condition exhibited the highest values of strain hardening exponent n and strength coefficient K, implying the greatest capacity for strain hardening under plastic deformation. Conversely, the lowest hardening potential was observed in specimens exposed to overaged conditions, where both n and K were significantly reduced. These findings underscore the strong dependence of strain hardening behaviour on the thermal exposure parameters applied during aging.

Keywords: AlSi9Cu1, Heat treatment, Strain hardening, Mechanical surface treatment

1. Introduction

Aluminium casting alloys of the Al-Si-Cu system, such as AlSi9Cu1, are widely used in the automotive and aerospace industries due to their favourable combination of low density, good castability, and satisfactory mechanical properties. However, their final performance strongly depends on the applied heat treatment, which influences the microstructure and, consequently, the mechanical response of the alloy.

In addition to heat treatment, the mechanical performance of aluminium alloys can be further improved by surface mechanical treatments such as roller burnishing, shot peening, or grit blasting. These processes are commonly employed to enhance surface integrity, increase fatigue resistance, and extend the service life of components [1-3]. Their effectiveness, however, strongly depends on the material's ability to undergo plastic deformation, as described by its flow behaviour.

Several strain-hardening laws, such as the Hollomon, Swift, Voce, and Ludwigson models, can describe the plastic response of metals [4]. These models differ mainly in how well they capture the initial curvature of the hardening curve or its saturation at large strains. In this study, the experimental data show a monotonic power-law type hardening without evident saturation, making the Hollomon law sufficiently accurate. Its simple two-parameter form also minimizes overfitting and ensures stable numerical implementation. Therefore, the Hollomon model was chosen as the most appropriate description of the material's hardening behavior [5,6].

The plastic response of the material is described by the Hollomon law, which uses the strain hardening exponent n and the strength coefficient K to characterize the flow behavior. These parameters characterize the ability of a material to distribute plastic deformation and resist localized necking. A higher value of n indicates an increased capacity for uniform plastic deformation prior to necking, which is closely related to ductility, formability and fatigue resistance. As the value of n increases, the

strengthening effect from shot peening or deep rolling also increases, the surface becomes harder and more resistant. The strength coefficient K represents the overall strength level of the material and is influenced by alloy composition, microstructure, and thermal history.

Both n and K are strongly affected by heat treatment, which modifies the microstructure of Al-Si-Cu alloys through changes in the morphology of silicon particles, precipitation of intermetallic phases, and redistribution of solute atoms. For example, solution treatment followed by artificial aging typically increases strength (K), while the effect on strain hardening capacity (n) depends on precipitate size and distribution [7,8]. Since higher strain hardening capacity enhances the material's response to surface treatments by enabling greater plastic strain accumulation and more stable compressive residual stresses, understanding the influence of heat treatment on n and K is essential for optimizing both bulk mechanical properties and surface performance. For most wrought aluminium alloys, the strain hardening exponent typically ranges between 0.2 and 0.4. This group includes, for example, Al-Mn alloys, Al-Mg alloys, and commercially pure aluminium. In the case of Al-Si and Al-Mg-Si based alloys, the strain hardening exponent is slightly lower, ranging from 0.15 to 0.35 [7,9,10].

Previous studies have investigated related questions for various aluminium alloys, providing useful context for the present work. Experimental and modelling efforts on wrought and casting Al-alloys have shown that heat-treatment state (e.g., solutionized, peak-aged, overaged) can markedly change K and, in many instances, n. In several precipitation-hardenable alloys, peak aging generally increases K but the influence on n may be non-monotonic and dependent on precipitate size, distribution and matrix hardening. Studies on both high-strength wrought alloys and cast alloys also indicate that overaging or coarsening of precipitates typically reduces work-hardening capacity and may diminish the beneficial effects of surface mechanical treatments [11-13]. Collectively, the literature suggests that tailoring heat-treatment parameters is a viable route to optimise an alloy's response to surface strengthening, but that specific outcomes are alloy- and process-dependent.

The present study focuses on the evaluation of how different heat treatment regimes affect the strain hardening behaviour of AlSi9Cu1 alloy, with emphasis on the variation of the strain hardening exponent n and the strength coefficient K, and on implications for the effectiveness of surface mechanical treatments.

2. Materials and methods

2.1. Experimental material

The experimental material used in this study is the AlSi9Cu1 alloy, which, due to its high Si content, is primarily intended for casting applications. The increased Cu content provides improved retention of mechanical properties at elevated temperatures and enables hardenability of the final components through heat treatment. The AlSi9Cu1 alloy is commercially employed in the production of internal combustion engine components. Owing to its high resistance to elevated operating temperatures, good ductility, and low susceptibility to linear shrinkage, it is predominantly used in the manufacture of cylinder heads for turbocharged diesel engines. The chemical composition of the experimental alloy, as determined from the inspection certificate, is given in Tab.1, while the mechanical properties of the as-cast material are presented in Tab.2.

Table 1.
Chemical composition of AlSi9Cu1 (wt.%)

Si	**Fe**	**Mn**	**Ni**	**Ti**
9.42	0.36	0.35	0.15	0.10
Cu	**Pb**	**Mg**	**Zn**	**Al**
1.20	0.07	0.22	0.40	bal.

Table 2.
Mechanical properties of AlSi9Cu1

AlSi9Cu1	**$R_{p0.2}$ (MPa)**	**R_m (MPa)**	**A_{50} (%)**
(F)* (K)**	175	230	7.80
*(F) – as cast; **(K) – cast into a metal mold			

The experimental material was gravity cast into a metallic mould preheated to 150 ± 5 °C. The pouring temperature of the melt was 740 ± 10 °C. Melting was carried out in a resistance furnace without the use of protective atmosphere or degassing procedures.

2.2. Heat treatment

The heat treatment consisted of solution annealing followed by artificial aging (designated as T6 according to ISO 3522), which is commonly applied to increase the yield strength, ultimate tensile strength, and hardness of the material. Solution annealing was carried out in a resistance furnace without protective atmosphere by heating to 530 ± 10 °C, followed by accelerated quenching in water at 80 ± 5 °C and subsequent cooling in air. The temperature profile of the solution annealing treatment is shown in Fig. 1.

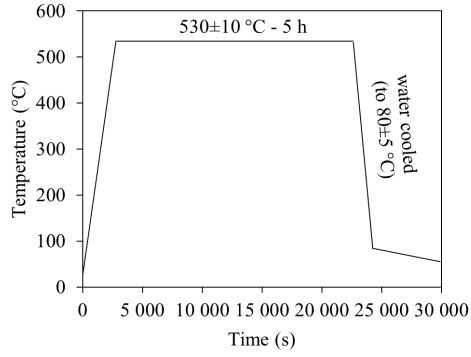

Fig. 1. Temperature profile of the solution annealing treatment of AlSi9Cu1

Artificial aging, which followed the solution annealing, was performed in a resistance furnace without protective atmosphere at temperatures of 160, 180, 200, and 240 °C, with soaking times of 4, 6.5, 8.5, and 10 h, followed by air cooling. The temperature profiles of the artificial aging treatments are shown in Fig. 2. Four specimens were subjected to each heat treatment cycle. In addition,

four specimens were taken after solution annealing only, without subsequent aging. In total, 68 test specimens were exposed to the complete heat treatment procedure.

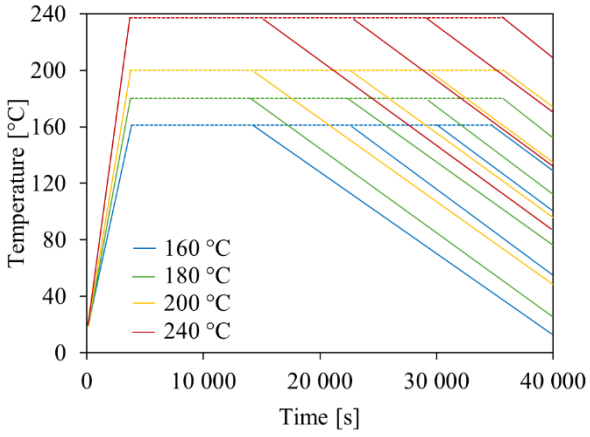

Fig. 2. Temperature profile of artificial aging of AlSi9Cu1

2.3. Static tensile test

Static tensile tests were performed on all specimens subjected to heat treatment. The geometry of the test specimens, which were machined from the castings, is shown in Fig. 3. The tests were conducted in accordance with the STN EN ISO 6892-1, with strain recorded during the entire test by means of an extensometer. The crosshead displacement rate was kept constant at 0.083 mm·s^{-1} for all specimens. Tensile test was performed on WDW20 tensile test device.

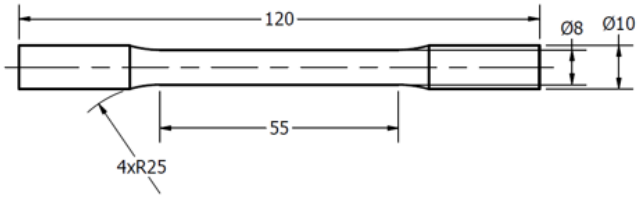

Fig. 3. Dimensions of tensile test specimens

2.4. Hardness test

Hardness was measured using the Brinell method (HBW) with a 2.5 mm wolfram carbide ball and a 187.5 kgf load applied for 10 s (HBW 2.5/187.5/10). For each sample, five individual indentations were performed, and the average value was taken as the final hardness. All measurements were carried out at the mid-thickness of the transverse section to ensure representative results.

2.5. Determination of the strain hardening exponent n and strength coefficient K

The strain hardening exponent was determined from the stress–strain (σ-ε) relationship obtained by static tensile test. To obtain relevant data for the calculation of the strain hardening exponent, the engineering stress–strain curve was converted into a true stress–true strain (σ_t-ε_t) curve using the following relations:

$$\sigma_t = \sigma \cdot (1 + \varepsilon) \tag{1}$$

$$\varepsilon_t = ln\,(1 + \varepsilon) \tag{2}$$

The strain hardening exponent n and the strength coefficient K were determined from the true stress–true strain (σ_t–ε_t) curve in the plastic deformation region, specifically between the yielding point and the onset of plastic instability (necking point). These parameters were obtained by fitting the experimental data to the Hollomon equation (3):

$$\sigma_t = K \cdot \varepsilon_t^{\,n} \tag{3}$$

where σ_t is the true stress, ε_t is the true strain, K is the strength coefficient, and n is the strain hardening exponent.

For data processing, the Hollomon equation (3) was linearized by applying a logarithmic transformation (4):

$$ln\,\sigma_t = ln\,K + n \cdot ln\,\varepsilon_t \tag{4}$$

The values of n and K were then determined by performing linear regression on the log σ_t – log ε_t data in the specified plastic deformation range, where the slope of the regression line corresponds to n and the intercept corresponds to ln K.

3. Results and discussion

By performing a static tensile test on heat-treated test specimens and subsequent data analysis, the values of the yield strength, tensile strength, and ductility of AlSi9Cu1 were obtained. Table 3 shows the mechanical properties of the AlSi9Cu1 alloy after T6 heat treatment.

Table 3.
Mechanical properties of heat treated samples of AlSi9Cu1

$R_{p0.2}$ (MPa)	160°C	180°C	200°C	240°C
4 h	205	315	308	238
6.5 h	230	326	299	252
8.5 h	274	285	280	202
10 h	282	309	294	188
R_m (MPa)	**160°C**	**180°C**	**200°C**	**240°C**
4 h	324	362	372	334
6.5 h	330	378	321	325
8.5 h	350	345	363	355
10 h	352	360	365	328
A_{50} (%)	**160°C**	**180°C**	**200°C**	**240°C**
4 h	6.6	2.4	1.7	1.9
6.5 h	4.3	2.1	2.5	1.7
8.5 h	1.5	1.2	2.4	2.0
10 h	2.1	2.2	1.8	1.2

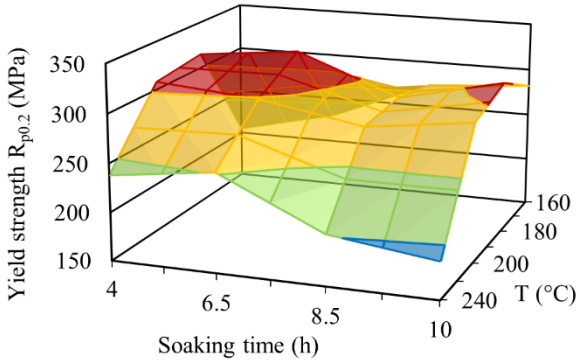

Fig.4 Yield strength of AlSi9Cu1 after T6 heat treatment

Fig.5 shows the microstructure of the AlSi9Cu1 alloy in the as-cast condition, characterized by a heterogeneous distribution of eutectic Si and intermetallic phases. In contrast, Fig.6 illustrates the microstructure after the T6 heat treatment (4 h at 160 °C), where the Si particles appear more spheroidized and the microstructure is noticeably refined. These changes confirm the expected microstructural evolution associated with artificial aging.

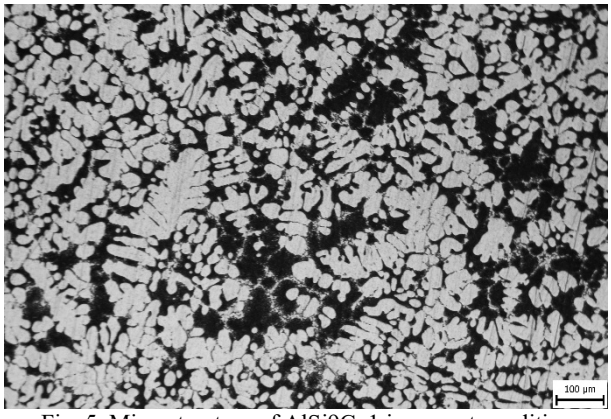

Fig. 5. Microstructure of AlSi9Cu1 in as-cast condition

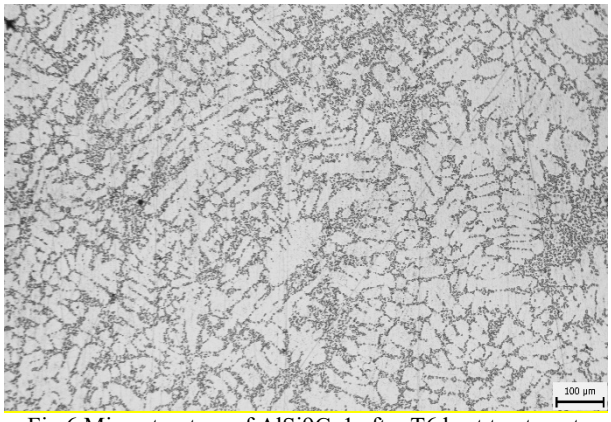

Fig.6 Microstructure of AlSi9Cu1 after T6 heat treatment.

Tab.4 shows the average values of strain hardening exponent n and strength coefficients K of samples subjected to solution annealing and artificial aging.

Table 4.
Values of n and K of heat treated samples of AlSi9Cu1.

n (-)	160°C	180°C	200°C	240°C
4 h	0.18	0.17	0.12	0.06
6.5 h	0.17	0.16	0.10	0.05
8.5 h	0.15	0.11	0.09	0.04
10 h	0.15	0.11	0.08	0.04
K (MPa)	**160°C**	**180°C**	**200°C**	**240°C**
4 h	619	684	576	387
6.5 h	616	619	527	391
8.5 h	570	589	522	368
10 h	562	544	501	351

For the specimens subjected only to solution annealing, without subsequent artificial aging, the strain hardening exponent was determined as n = 0.22 and the strength coefficient as K = 716 MPa. Yield strength of AlSi9Cu1 after solution heat treatment was 191 MPa.

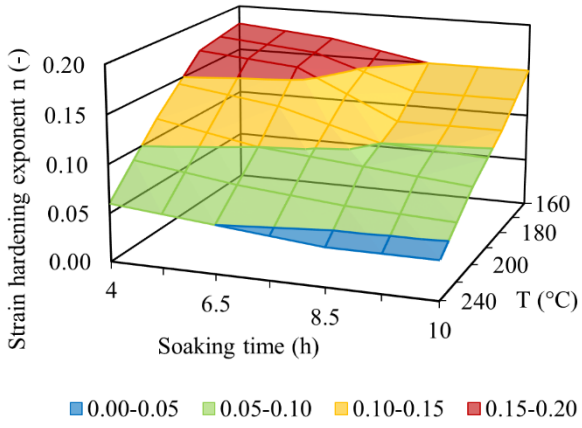

Fig. 4. Strain hardening exponent of AlSi9Cu1 after heat treatment

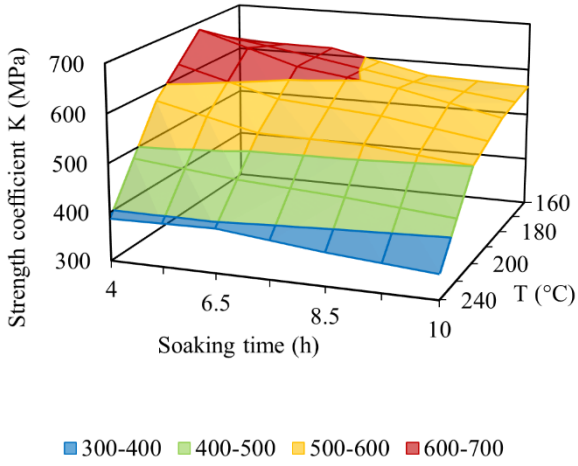

Fig. 5. Strength coefficient of AlSi9Cu1 after heat treatment

From the above values, it can be observed that with increasing artificial aging temperature and soaking time, the value of the strain hardening exponent decreases significantly. Compared to the state after solution annealing, a decrease of up to 80% can be observed.

The hardness values obtained from Brinell testing are summarized in Tab.5. These values show good agreement with the measured mechanical properties, specifically the yield strength, strength coefficient K, and strain hardening exponent n, confirming the internal consistency of the experimental results.

Table 5.
Hardness values of AlSi9Cu1 after T6 heat treatment

HBW 2.5/187.5/10	160°C	180°C	200°C	240°C
4 h	127	124	122	95
6.5 h	119	123	112	86
8.5 h	120	128	112	75
10 h	101	122	111	78

4. Conclusions

The experimental results demonstrate a clear decreasing trend in both the strain hardening exponent n and the strength coefficient K with increasing temperature and duration of artificial aging. While direct microstructural evidence was not obtained in this study, the observed behaviour is consistent with well-established mechanisms in Al–Si–Cu alloys. At lower aging temperatures and shorter times, a fine and relatively homogeneous distribution of precipitates is typically expected, which can hinder dislocation motion and enhance both strength and strain hardening capacity. Conversely, extended or high-temperature aging is generally associated with precipitate coarsening and a reduction in their number density, which reduces the ability of the material to accumulate dislocations during plastic deformation. Such microstructural processes, reported in the literature, provide a plausible explanation for the observed reduction in n and K.

From a practical perspective, these findings are highly relevant for surface mechanical treatments such as shot peening and roller burnishing, which rely on the introduction of controlled plastic deformation in the near-surface region. A higher strain hardening exponent n promotes more uniform distribution of plastic strain and stabilizes compressive residual stresses, thereby enhancing fatigue resistance. Similarly, a higher strength coefficient K reflects the material's ability to sustain greater stresses during surface plastic deformation. As a result, specimens exhibiting higher n and K values are expected to respond more effectively to surface strengthening treatments, accumulating greater beneficial residual stresses and improved resistance to crack initiation.

In contrast, overaged conditions characterized by reduced n and K values limit the efficiency of surface mechanical treatments. In these cases, the alloy exhibits reduced work-hardening capability and a diminished ability to sustain compressive residual stresses induced by peening or burnishing. This suggests that optimal aging conditions should be carefully tailored not only to maximize bulk strength but also to preserve sufficient strain hardening capacity, thereby ensuring maximum benefit from subsequent surface modification processes.

Acknowledgements

This research was supported by the Cultural and Educational Grant Agency of the Ministry of Education of the Slovak Republic under project No. KEGA 018ŽU-4/2025; and by the Scientific Grant Agency of the Ministry of Education, Science, Research and Sport of the Slovak Republic under project VEGA 1/0044/22. Funded by the EU NextGenerationEU through the Recovery and Resilience Plan for Slovakia under the project No. 09I03-03-V05-00002.

References

[1] Chih-Hang, S., Tai-Cheng C., Yi-Shiun D., Guan-Xun L. & Leu-Wen, T. (2023). Effects of micro-shot peening on the fatigue strength of anodized 7075-T6 alloy. *Materials*. 16(3), 1160, 1-13. DOI: 10.3390/ma16031160.

[2] Świetlicki, A., Szala, M. & Walczak, M. (2022). Effects of shot peening and cavitation peening on properties of surface layer of metallic materials—a short review. *Materials*. 15(7), 2476, 1-26. DOI: 10.3390/ma15072476.
[3] Thang, W., Lv, S., Yao, L., Tong, X. & Li, B. (2014). Influence of shot peening intensity on residual strength of aluminium alloy. *Materials Research Innovations*. 19(8), 541-544. DOI: 10.1179/1432891715Z.0000000001744.
[4] Joun, M.-S., Razali, M.K., Jee, C.-W., Byun, J.-B., Kim, M.-C. & Kim K.-M. (2022). A review of flow characterization of metallic materials in the cold forming temperature range and its major issues. *Materials*. 15(8), 2751, 1-32. DOI: 10.3390/ma15082751.
[5] Nutor, R.K., Adomako, N.K. & Fang, Y.Z. (2017). Using the hollomon model to predict strain-hardening in metals. *American Journal of Materials Synthesis and Processing.* 2, 1, 1-4.
[6] Hollomon, J.H. (1945). Tensile Deformation. *Transactions of the Metallurgical Society of AIME*. 162, 268-290.
[7] Totten, G.E. & MacKenzie, D.S. (2003). *Handbook of Aluminum: Volume 1 – Physical Metallurgy and Processes.* (1st. ed.). New York, NY: Marcel Dekker.
[8] Wang, Q. & Cáceres, C. (1997). On the strain hardening behaviour of Al-Si-Mg casting alloys. *Materials Science and Engineering A*. 234-236, 106-109. DOI: 10.1016/S0921-5093(97)00207-4.
[9] Khelfa, T., Muñoz-Bolaños, J.A., Li, F., Cabrera-Marrero, JM. & Khitouni, M. (2020). Strain-Hardening Behavior in an AA6060-T6 Alloy Processed by Equal Channel Angular Pressing. *Advanced Engineering Materials*. 23(1), 2000730, 1-11. DOI: 10.1002/adem.202000730.
[10] Bátorfi, J.G., Pál, G., Chakravarty, P. & Sidor, J.J. (2023). Assessment of Deformation Flow in 1050 Aluminum Alloy by the Implementation of Constitutive Model Parameters. *Applied Sciences*. 13(7), 4359, 1-17. DOI: 10.3390/app13074359.
[11] Dash, S.S. & Chen, D. (2023). A review on processing–microstructure–property relationships of Al-Si alloys: recent advances in deformation behavior. *Metals*. 13(3), 609, 1-64. DOI: 10.3390/met13030609
[12] Lagalante, I., Martucci, A., Manfredi D.G., Fino, P. & Lombardi, M. (2025). Tailoring mechanical properties of AlSi9Cu3(Fe) alloy via heat treatments in PBF-LB Processing. *Materials & Design*. 258, 114591, 1-17. DOI: 10.1016/j.matdes.2025.114591
[13] Meyers, M.A. & Chawla, K.K. (2008). *Mechanical Behavior of Materials*. (2nd ed.). Cambridge: Cambridge University Press.